DOI: 10.1002/ejic.200900728

Optically Active Polyoxotungstates Bearing Chiral Organophosphonate Substituents

Mauro Carraro,*[a] Gloria Modugno,[a] Andrea Sartorel,[a] Gianfranco Scorrano,[a] and Marcella Bonchio*[a]

Keywords: Polyoxometalates / Chirality / Organic–inorganic hybrid composites / Phosphorus / Circular dichroism

Divacant Keggin-type polyoxotungstates $[\gamma\text{-}XW_{10}O_{36}]^{8-}$ with X = Si or Ge, were functionalized with chiral phosphoryl groups. The hybrid compounds $[(R^*PO)_2(\gamma\text{-}XW_{10}O_{36})]^{4-}$ with R = *N*-protected aminoalkyl groups or *O*-protected amino acid derivatives, were isolated. The solution characterization of the products was performed by different techniques: ^{183}W, ^{31}P, ^{13}C, and ^{1}H NMR spectroscopy, electrospray ionization mass spectrometry, UV/Vis spectroscopy, and circular dichroism (CD). The experimental data confirm the covalent grafting of the organic moieties onto the polyanionic surface. A chirality transfer, from the pendant organic arm to the inorganic framework is apparent from CD studies. Multiple Cotton effects were observed in the region of charge-transfer transitions pertaining to W–O bonds. Furthermore, the ^{183}W NMR spectra are consistent with the expected C_2 symmetry, resulting from introduction of two organic stereocenters. The title complexes were used in the presence of hydrogen peroxide to perform the oxidation of methyl *p*-tolyl sulfide. Implications for the design of enantioselective catalysts based on these derivatives are discussed.

Introduction

Polyoxometalates (POMs) are inorganic and discrete multimetal clusters; they have found applications in catalysis, material sciences, and medicine.[1–7] Their properties may be modified depending on the elemental composition, structure, and countercations.[1] In addition, the presence of organic substituents anchored on the POM surface offers the possibility to tune the stereoelectronic features of the resulting complexes, as well as their solubility, reactivity, and hydrolytic stability.[4,8,9] The merging of organic and inorganic domains is a developing field of investigation focusing on the design of new hybrid materials.[10] In this respect, surface-appended organic moieties carrying suitable functional groups are introduced to foster the extended organization of the POM molecular units.[7,11,12] This strategy was successfully employed to obtain polymerizable,[13] dendrimeric,[14] and supramolecular derivatives.[15] Moreover, a tailored hybrid modification of POMs is instrumental for their grafting onto surfaces and onto nanoparticles,[16] for their embedding into polymeric membranes,[17] and for the introduction of organic or organometallic residues for advanced catalytic applications.[18,19] As a result of the potential applications of POMs in medicine, the preparation of hybrid derivatives is also of interest to introduce molecular recognition sites while increasing their bioavailability.[6,20]

Within this scenario, the upgrade towards chiral POM-based complexes and materials is highly desirable for both biomedical applications[21] and stereoselective catalysis.[22] Totally inorganic, chiral POMs have been described in the literature.[23] However, resolution of the enantiomeric structures is hampered by racemization through water exchange, partial hydrolysis, or fluxional behavior so that only in a few cases has spontaneous resolution of the enantiopure conglomerates been successfully obtained.[24–26] Therefore, an alternative strategy is based on the direct attachment of chiral organic groups onto the POM surface.[27–29] Chiral POM-based hybrids have been obtained by tailoring the organic–inorganic structures and their intermolecular junctions, also including other transition-metal ions to bridge the molecular building units.[30] Interestingly, the assembly into an extended enantiomorphous structure has also been obtained in the absence of any chiral auxiliary component.[31] As a further remark, optically active hybrid materials, like chiral molecular magnets and conductors, have been prepared by following analogous synthetic approaches.[32]

Stable diastereomeric derivatives have been obtained with organostannanes grafted onto monovacant Wells–Dawson polyoxotungstates to link amino acids or chiral amines,[33] or with binaphtholic derivatives grafted onto hexamolybdate Lindqvist structures through Mo–N bounds.[34] The interplay of multidentate organic ligands

[a] ITM-CNR and Department of Chemical Sciences, University of Padova,
via F. Marzolo 1, 35131 Padova, Italy
Fax: +39-049-8275239
E-mail: mauro.carraro@unipd.it
marcella.bonchio@unipd.it

Supporting information for this article is available on the WWW under http://dx.doi.org/10.1002/ejic.200900728.

with transition-metal-substituted POMs has been described, as in the case of a dimeric Zr^{IV}-substituted Wells–Dawson polyoxotungstate containing tartaric acid.[35,36] As a corollary, the use of chiral cations has been explored to prepare optically active peroxopolyoxotungstates.[37,38] We recently contributed to this field by preparing chiral Strandberg-type pentamolybdates functionalized with aminoalkylphosphonates. These compounds behave as molecular gelators in hydroalcoholic solutions, where they assemble into nanostructured twisted fibrils. The induced helicity of the hybrid fibrils results from the expression of chirality at the supramolecular level.[12]

We present herein the synthesis and characterization of new chiral polyoxotungstophosphonates, in enantiopure form, derived from the covalent functionalization of lacunary Keggin-type precursors.

The resulting complexes display high hydrolytic stability, which is a precise requirement for their further use as material building blocks and/or as catalysts in oxygen transfer reactions, in combination with hydrogen peroxide as bulk oxidant.[58]

Results and Discussion

The synthetic routes to Keggin-type polyoxotungstates functionalized with chiral phosphonates are depicted in Scheme 1. In both cases, a divacant POM complex featuring a surface defect is used as precursor with the aim to exploit the oxygen atoms of the lacunary site, which are prone to react with electrophilic reagents such as organophosphonic acids. The organic residue was directly introduced as chiral *N*-protected aminophosphonate (Scheme 1, pathway a) or by the sequential amino acid coupling on a phosphonoacetic-substituted POM (Scheme 1, pathway b). The grafting reaction occurs in acetonitrile, under phase-transfer conditions, fostering the dissolution of the POM with nBu$_4$NBr.[39] By using a similar protocol, decoration of the lacunary $[\gamma\text{-SiW}_{10}O_{36}]^{8-}$ unit was reported to provide hybrid POMs with two surface-anchored organophosphonate (RPO^{2+}) groups facing each other while linked to two oxygen atoms of two edge-shared WO_6 octahedra. This structural arrangement was shown by solid-state X-ray characterization.[39] The new compounds display very similar UV/Vis and FTIR spectra (Figure 1), thus suggesting the same substitution pattern. The solution characterization of the resulting hybrid POMs was also performed by the following techniques: ^{183}W, ^{31}P, ^{13}C, and ^{1}H NMR spectroscopy, electrospray ionization (ESI) mass spectrometry (MS), and circular dichroism (CD).[40] CD spectroscopy, in particular, has been used as a tool to assess the chirality transfer from the organic moiety to the POM scaffold.[41] Moreover, geometry optimization of the products has been computed by DFT (BP86 functional, TZ2P basis set), including relativistic and solvent effects, to assess the spatial distribution of the organic pendant arm, evaluating the impact of hydrogen bonding and steric effects on the stability of different conformers.

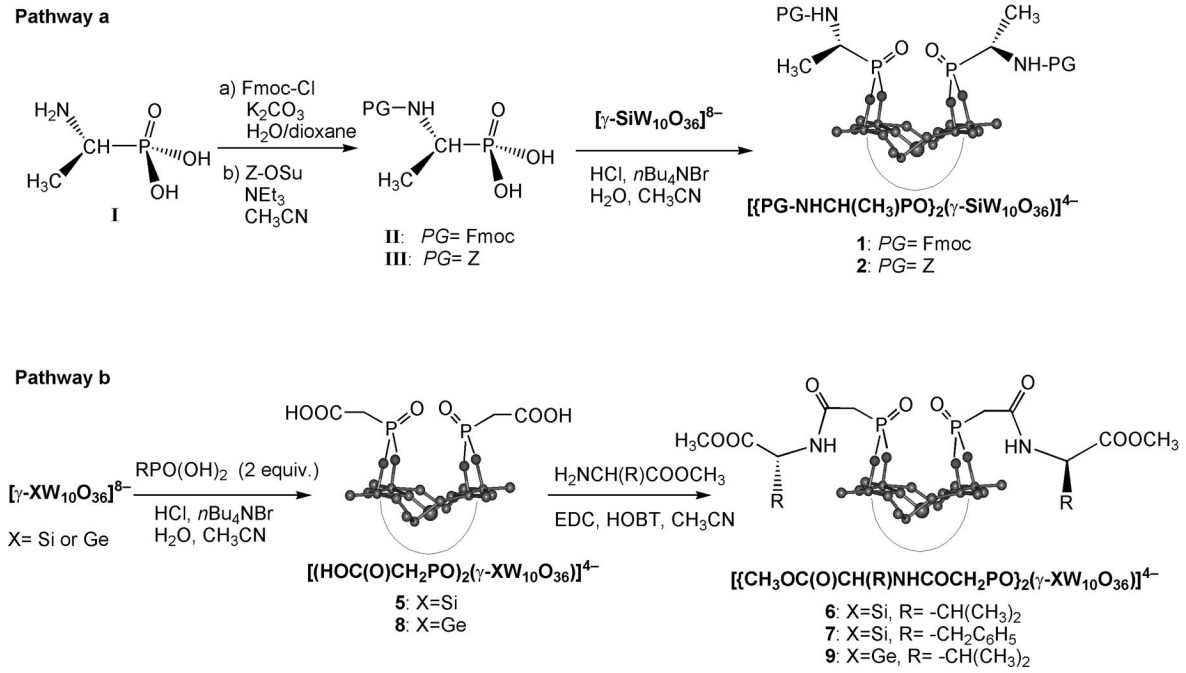

Scheme 1. Synthetic routes to Keggin-type polyoxotungstates functionalized with chiral phosphonates. Pathway a: grafting of *N*-protected aminoethyl phosphonic acids; pathway b: grafting of *O*-protected amino acids.

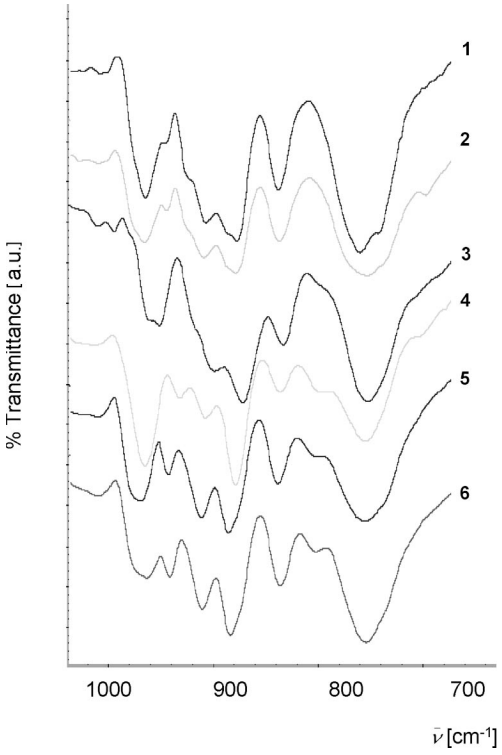

Figure 1. FTIR (KBr) spectra of POMs **1**–**6** in the region of W–O and P–O absorptions.

Grafting of *N*-Protected Aminoethyl Phosphonic Acids onto the POM (Scheme 1, Pathway a)

The unprotected aminoethylphosphonic acid (**I**) is hardly soluble in the reaction mixture, thus preventing careful control of the stoichiometry of the reagent. Moreover, the zwitterionic form of the organic reagent is likely associated as a counterion to the POM precursor. For these reasons, the aminoalkyl phosphonic acids were protected at the amino functions before reaction with the POM derivative. 9-Fluorenylmethoxycarbonyl (Fmoc) and benzyloxycarbonyl (Z) were thus introduced as protecting groups (PGs) with the aim to explore orthogonal deprotection procedures. The corresponding organophosphonic acids Fmoc-NHCH-$(CH_3)PO(OH)_2$ (**II**) and Z-$NHCH(CH_3)PO(OH)_2$ (**III**) were isolated and characterized (Scheme 1). The substitution reaction on the lacunary site of $[\gamma\text{-}SiW_{10}O_{36}]^{8-}$ occurs smoothly to provide $TBA_3K[\{C_{13}H_9CH_2OC(O)NHCH(CH_3)PO\}_2(\gamma\text{-}SiW_{10}O_{36})]$ (**1**) and $TBA_3K[\{C_6H_5CH_2OC(O)NHCH(CH_3)PO\}_2(\gamma\text{-}SiW_{10}O_{36})]$ (**2**) in 83 and 63% yield, respectively.

Table 1 collects the characterization data for the phosphonic acid precursors **I**–**III** and for the POM-based hybrids. ^{31}P NMR spectroscopy is a convenient tool for monitoring the reaction, as separate resonances are observed for both starting reagents and POM-based phosphonates (Table 1). Moreover, a single ^{31}P NMR signal is indicative of a single product with a symmetric substitution at the POM lacunary site. The chemical shifts of the starting reagents are affected by the introduction of PGs and by subsequent grafting onto the POM surface. In particular, a downfield shift ($\Delta\delta$ = 8.3–10 ppm) was observed for the phosphorus signal of both compounds **II** and **III** with respect to **I**, in agreement with the deshielding effect of the amido group, whereas a smaller upfield shift ($\Delta\delta$ = 1.4–2.6 ppm) was observed upon grafting of **II** and **III** onto the inorganic surface to give **1** and **2** (Table 1).

^1H NMR spectroscopy rules out the occurrence of any undesired deprotection pathway during the anchoring process, as the expected resonances for the aromatic PGs are observed between 7.8–7.3 and 7.4–7.3 ppm for hybrid POMs **1** and **2**, respectively. The ESI mass spectra of hybrids **1** and **2**, registered in negative mode, shows clusters centered at *m*/*z* = 1020 and 965 attributed, respectively, to the ions $[H\{C_{13}H_9CH_2OC(O)NHCH(CH_3)PO\}_2(\gamma\text{-}SiW_{10}O_{36})]^{3-}$ and $[H\{C_6H_5CH_2OC(O)NHCH(CH_3)PO\}_2(\gamma\text{-}SiW_{10}O_{36})]^{3-}$. FTIR evidences diagnostic bands at 760, 880, and 905 cm^{-1} for $\nu_{as}(W\text{–}O_b\text{–}W)$ and weak bands at 1100–1200 cm^{-1} for $\nu_{as}(P\text{–}O)$ for both derivatives, confirming the integrity of the POM structure (Figure 1).[39]

Hybrids **1** and **2** exhibit a ^{183}W NMR spectral pattern in agreement with the expected bis-functionalized, C_2-symmetric structure, with three multiple resonances with relative intensity 1:2:2, corresponding to W_C (two side atoms), W_A (four bottom tungsten atoms), and W_B (four vacant W atoms; Table 1 and Figure 2).

Table 1. ^{31}P NMR, ^{183}W NMR, and MS (ESI–) data for the organophosphonic acids and their corresponding hybrid polyoxometalate derivatives in CH_3CN solutions.

Compound	^{31}P NMR, δ [ppm]	^{183}W NMR, δ [ppm]	ESI-MS, *m*/*z*[e]
I	14.1[a]	–	nd
II	22.4	–	nd
III	24.1[b]	–	nd
1	21.0	–103.1, –111.9, –113.2, –145.1[d], –145.2[d]	1020
2	21.5	–105.9, –114.7, –115.8–147.8[d]	965
3	18.8	–[c]	nd
5	17.5	–107.0, –115.6, –156.9[d]	884
6	19.7	–[c]	961
7	19.8	–[c]	993
8	17.6	–81.7, –97.6, –132.0[d]	900
9	19.2	–79.4, –97.8, –97.9, –126.2[d]	975

[a] In D_2O. [b] In $CD_3CN/[D_6]DMSO$. [c] No signals observed due to paramagnetism of the species. [d] Doublets. [e] MS (ESI–) signals corresponding to the HM^{3-} ions. nd = not determined.

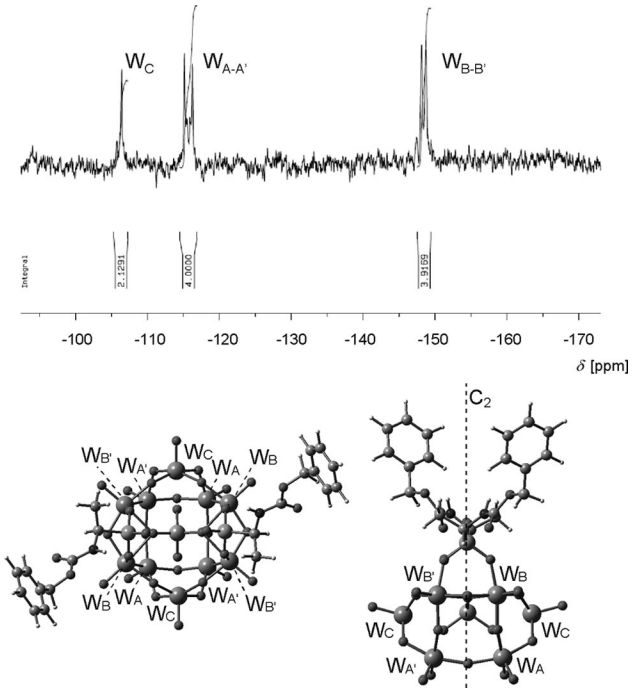

Figure 2. Top: ^{183}W NMR of **2**; bottom: representation of **2**, top and lateral view, highlighting diastereotopic W ions. The C_2 symmetry axis crosses the silicon atom.

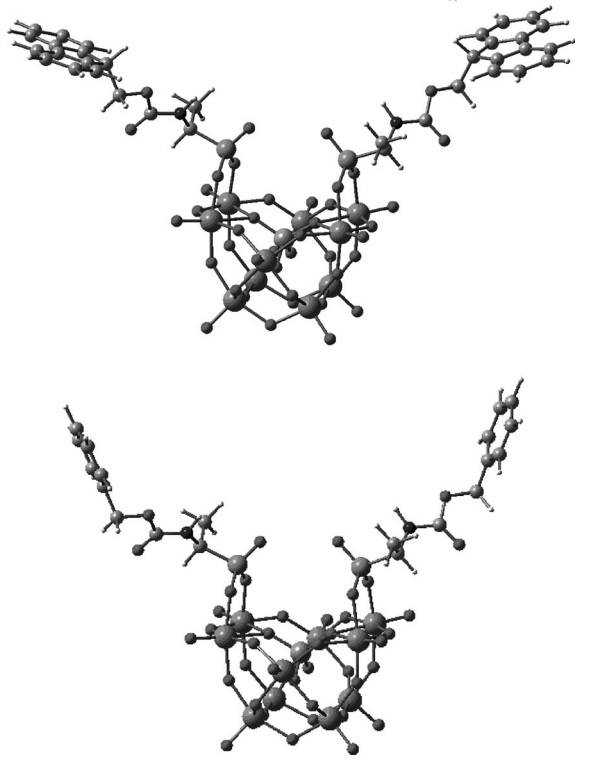

Figure 3. Optimized geometries of **1** (top) and **2** (bottom).

The most-shielded signals (W_B) appear as doublets because of the heteronuclear phosphorus–tungsten coupling ^2J(W,P) of 9.0 Hz (for **1**) and 9.7 Hz (for **2**). In addition, a splitting of the signals was observed for **1** and **2** with respect to the parent [γ-$SiW_{10}O_{36}$]$^{8-}$. Heteronuclear NMR has already been reported to reveal diastereomeric interaction occurring between amino acids and chiral polyanionc scaffolds.[33,42,43] In this case, however, the diastereotopic atoms belong to enantiopure species. The optimized geometries of POMs (*S*,*S*)-**1** and (*S*,*S*)-**2** (Figures 2 and 3) nicely illustrate how the chiral substituents, related by C_2 symmetry, may be oriented on the inorganic unit, thus leading to the removal of the equivalence of the W_B and W_A atoms; these atoms become pairs of diastereotopic atoms (W_A and W_A', W_B and W_B'). Noteworthy, a larger splitting was observed for the remote W_A and W_A' ions (about 1.2 ppm), suggesting that a significant perturbation involves the whole structure. POM **1** presents a very small splitting (δ = 0.1 ppm) of the upfield doublet, thus allowing the W_B and W_B' signals to be distinguished. The W_C atoms, finally, are still chemically equivalent, but their strong chemical downfield shift (>80 ppm) with respect to the signal of [γ-$SiW_{10}O_{36}$]$^{8-}$ is in agreement with a deep overall electronic change of the bis-functionalized structure, mainly affecting nonvacant W atoms.

Both (*R*,*R*) and (*S*,*S*) enantiomers of **1** and **2** were prepared upon functionalization of [γ-$SiW_{10}O_{36}$]$^{8-}$ with the two enantiomers of the aminoethylphosphonic acid, properly protected with Fmoc or Z groups. As expected, the two enantiomers of hybrids **1** and **2** show mirror-symmetric CD spectra. In addition, **1** and **2** exhibit similar chiroptical behavior, with the same number of exciton splittings and Cotton effects, at similar wavelengths: 230 (2.8×10^4), 251 (-1.0×10^4), 267 (1.3×10^4), 289 (-1.3×10^4), and 315 nm (1.1×10^4 deg cm^2 dmol^{-1}) for (*S*,*S*)-**1** and 228 (2.7×10^4), 251 (-9.7×10^3), 271 (1.1×10^4), 288 (-5.9×10^3), and 314 nm (1.5×10^4 deg cm^2 dmol^{-1}) for (*S*,*S*)-**2** (Figure 4). The lower optical activity observed for the protected phosphonic acids [a single positive Cotton effect at 266 nm with $\theta = 5.8\times10^3$ deg cm^2 dmol^{-1} for (*R*)-**II** and at 212 nm with $\theta = 1.7\times10^3$ deg cm^2 dmol^{-1} for (*S*)-**III**] in the spectral region where the characteristic oxygen-to-tungsten charge-transfer bands of the polyanion absorbs (Figure 4, inset) suggests that the optical activity is induced through chirality transfer. The CD spectra resulting from a similar exciton coupling of the chromophoric groups are also in agreement with the occurrence of analogous structural/electronic features for compounds **1** and **2**.

The possibility to remove the PGs in **1** and **2** was explored. The presence of unprotected amino groups is of interest to access further functionalizations, as well as to promote intra- and intermolecular ionic-type hydrogen bonds, arising from protonation equilibria. These latter can be exploited for the development of new POM-based extended assemblies.[12] Thus, the protecting groups in **1** and **2** were removed by using classic procedures: **1** was treated with diethylamine (Scheme 2, pathway a) to obtain [{$NH_2CH(CH_3)PO$}$_2$(γ-$SiW_{10}O_{36}$)]$^{4-}$ (**3**), whereas **2** was reduced with H_2 by using a Pd/C catalyst (Scheme 2, pathway b) to yield the corresponding reduced heteropolyblue [{$NH_2CH(CH_3)PO$}$_2$(γ-$SiW_{10}O_{36}$)]$^{n-}$ ($n > 4$; **4**). The ^{31}P

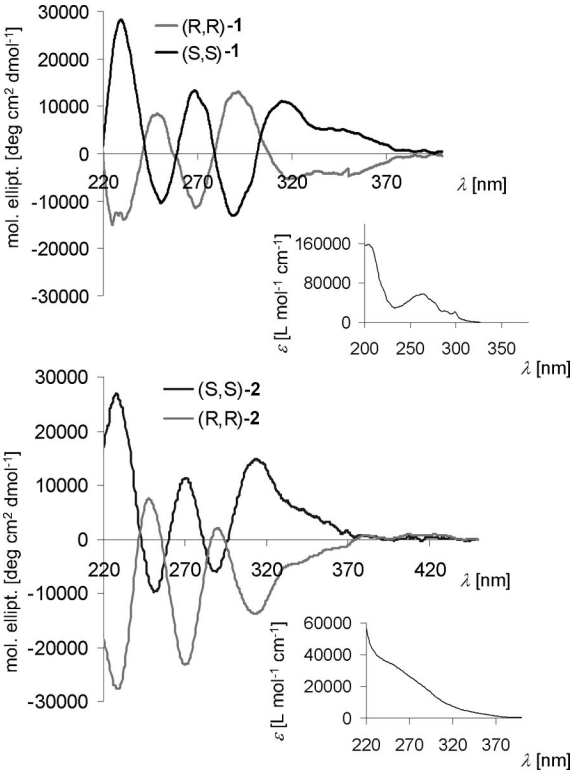

Figure 4. Circular dichroic spectra and UV/Vis (inset) spectra of complex **1** (top) and **2** (bottom) in CH_3CN.

NMR spectrum of **3** evidences a single peak at δ = 18.8 ppm ($\Delta\delta$ = –2.2 ppm with respect to **1**) as expected upon deprotection. Removal of the PGs was also confirmed by ^{1}H NMR spectroscopy (see Supporting Information).[44]

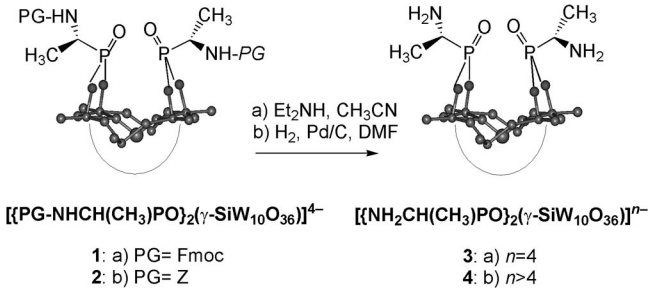

Scheme 2. Deprotecting procedures for the removal of the PGs from **1** and **2**.

The retention of the inorganic framework in **3** and **4** was confirmed by FTIR, where the main spectral features of the POM between 700 and 1000 cm^{-1} are maintained (Figure 1 and Supporting Information); moreover, the very weak absorption of the aromatic C–H bonds at 3065–3035 cm^{-1} and the C=O signal at 1719 cm^{-1} originally observed in **1** disappear, whereas amino N–H bending at 1634–1616 cm^{-1} is observed. The optimized geometry of **3** is represented in Figure 5.

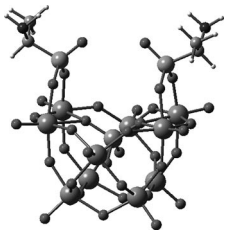

Figure 5. Optimized geometry of **3**.

Compared to parent complex **1**, **3** presents a lower UV/Vis absorption (Figure 6, top, inset), as well as a smaller number of exciton splittings, as expected upon removal of the chromophores (the aromatic moieties and the amido bonds). (*S*,*S*)-**3** presents the following Cotton effects: 237 (1.1×10^4), 271 (-9.9×10^3), 300 nm (2.2×10^3 deg cm^2 dmol^{-1}; Figure 6, top).

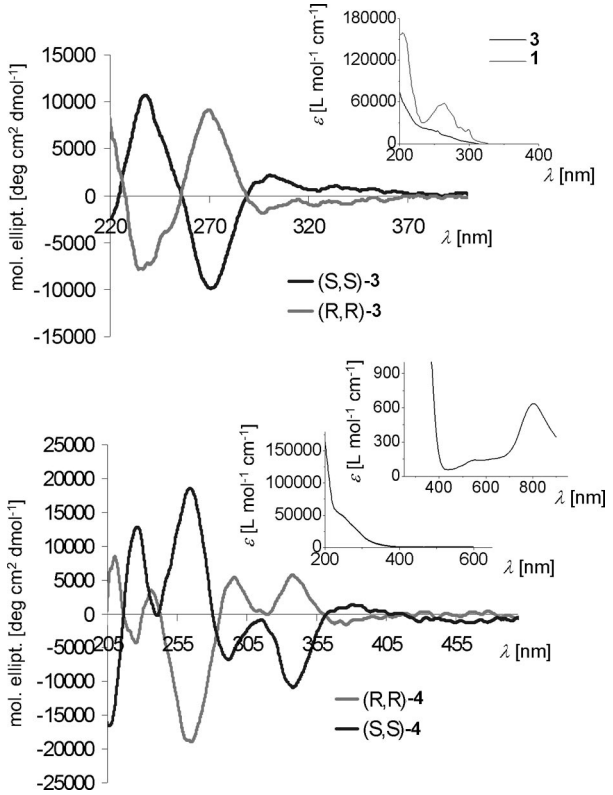

Figure 6. Top: CD spectrum of **3** with its UV/Vis spectrum compared to that of **1** (inset); bottom: CD spectrum of **4** with its UV/Vis spectrum (inset).

As a result of its reduced form, **4** is blue and presents a UV/Vis absorption up to 400 nm, with a small band at 800 nm (Figure 6, bottom, inset). This heteropolyblue complex exhibits a higher number of dichroic bands, with a small shift toward visible wavelengths. (*S*,*S*)-**4** presents the following Cotton effects: 227 (1.3×10^4), 264 (1.9×10^4), 292 (-6.8×10^3), 338 (-1.1×10^4), 381 nm (1.3×10^3 deg cm^2 dmol^{-1}). To the best of our knowledge, this is the first example of an induced circular dichroism pertaining to a chiral heteropolyblue POM. In this highly reduced form, the electrons, besides affecting spectroscopic properties, may also

increase the overall charge density affecting the proton/cation equilibria.[45] This observation opens up the possibility to obtain chiroptical switches with redox-dependent activity.[46]

Grafting of *O*-Protected Amino Acids (Scheme 1, Pathway b)

Elongation of the chiral pendant arm on the POM surface was addressed by reaction of the intermediate $[\{HOC(O)CH_2PO\}_2(\gamma\text{-}SiW_{10}O_{36})]^{4-}$ (**5**). Complex **5** was isolated and characterized in solution. The ^{183}W NMR spectrum shows peaks at –107.0, –115.6, and –156.9 ppm, with $^2J(W,P)$ = 11.4 Hz for the latter W_B signals. The $^{31}P\{^1H\}$ NMR spectrum presents a single resonance at δ = 17.5 ppm, whereas the bis-functionalization was confirmed by mass spectrometry (ESI–), by which the tricharged ion $[H\{HOC(O)CH_2PO\}_2(\gamma\text{-}SiW_{10}O_{36})]^{3-}$ with m/z = 884 was detected. Amino acid methyl esters can be covalently linked to **5** by means of classic condensation reactions. L-Valine was chosen as a model, as it is quite sterically hindered and does not contain functional groups that could affect the reaction. Ethyl-γ-dimethylaminopropylcarbodimmide (EDC) and 1-hydroxy-1,2,3-benzotriazole (HOBT) were used as dehydrating and activating agents, respectively. Despite the formation of byproducts originating from EDC, we used this reagent instead of DCC to obtain a higher reaction yield.[33,47] The related product, $[\{CH_3OC(O)CH[CH(CH_3)_2]NHCOCH_2PO\}_2(\gamma\text{-}SiW_{10}O_{36})]^{4-}$ (**6**) was isolated. The $^{31}P\{^1H\}$ NMR spectrum shows a single resonance at δ = 19.7 ppm, with a downfield shift of 2.2 ppm with respect to **5**, whereas the ^1H and ^{13}C NMR spectra confirm the presence of L-valine. The mass spectrum (ESI–) presents a cluster centered at m/z = 961, resulting from the $[H\{CH_3OC(O)CH[CH(CH_3)_2]NHCOCH_2PO\}_2(\gamma\text{-}SiW_{10}O_{36})]^{3-}$ ion.

Differently from **1**–**4**, the pendant arm in **6** features the approach of the amido group to the nucleophilic oxygen atoms of the inorganic framework, thus fostering the formation of two hydrogen bonds between the NH moieties and the W–O–W bridging oxygen atoms of the polyoxometalate (Figure 7). These favorable interactions account for a stabilization of 16 kcal mol^{-1} with respect to a conformer in which the amido groups are opposite to the POM domain. A stabilization energy of 8 kcal mol^{-1} falls in the typical range for a neutral donor–acceptor hydrogen bond,[2b] confirming that, despite the polyanionic charge of the POMs, the local charge distribution on the oxygen atoms is relatively low. Hydrogen bonding is a key tool for POM stabilization in the catalytic activation of hydrogen peroxide[2b] and/or evolving in supramolecular architectures.[12] In this respect, the design of suitable H-bonding patterns can boost the chirality transfer from the organic pendant arm to the inorganic envelope of the polyoxometalate through multiple noncovalent interactions.

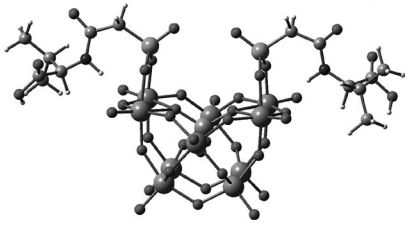

Figure 7. Optimized geometry of **6**.

The CD spectrum of **6** ($\theta_{max} = 1.1 \times 10^4$ deg cm^2 dmol^{-1} at 202 nm and 8.2×10^3 deg cm^2 dmol^{-1} at 215 nm) partially overlaps the signal of L-valine, which presents a similar positive Cotton effect below 230 nm ($\theta = 6.9 \times 10^3$ deg cm^2 dmol^{-1} at 210 nm), indicating that the chiral core on the organic moiety is not significantly altered after attachment to the POM (Figure 8).

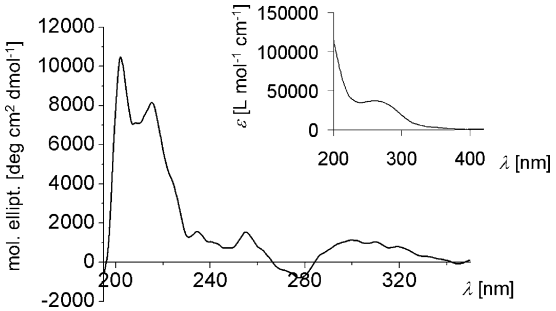

Figure 8. CD and UV/Vis (inset) spectra of **6**.

The reaction has shown to be of general scope, as L-phenylalanine was also grafted onto **5** to give $[\{CH_3OC(O)CH(CH_2C_6H_5)NHCOCH_2PO\}_2(\gamma\text{-}SiW_{10}O_{36})]^{4-}$ (**7**). Phosphonoacetic acid gives bis-functionalized products also with $[\gamma\text{-}GeW_{10}O_{36}]^{8-}$, leading to $[\{HOC(O)CH_2PO\}_2(\gamma\text{-}GeW_{10}O_{36})]^{4-}$ (**8**), which was coupled with L-valine by following the same reaction procedure to give $[\{CH_3OC(O)CH[CH(CH_3)_2]NHCOCH_2PO\}_2(\gamma\text{-}GeW_{10}O_{36})]^{4-}$ (**9**). In **7** and **9**, the ^{31}P NMR signals are downfield shifted ($\Delta\delta$ = 1.6–2.2 ppm) with respect to their parent complexes **5** and **8**, bearing the free carboxylic function. Analysis by MS (ESI–) confirms the introduction of the two amino acid arms, whereas the ^{183}W NMR spectrum of **9** presents the expected distinct signals for diastereotopic W_B, W_B' and W_A,W_A' atoms (Table 1).[48]

Catalytic Oxidations by Chiral POM Hybrids

Catalytic protocols using hydrogen peroxide as terminal oxidant, and involving competent W^{VI} peroxides, are generally characterized by negligible decomposition pathways and good to excellent selectivity. In this light, interesting results have been obtained with vacant POMs[2,49,50] and with their hybrid derivatives.[5,51] These latter display stable structures under multioxidation turnovers.

Thus, the enantioselective oxidation of methyl *p*-tolyl sulfide with H_2O_2 (Scheme 3) was used as a probe to obtain insight into the structural requirements of the chiral POM

catalysts. Table 2 reports the results obtained with complexes **1**–**6**, compared in terms of yield and enantiomeric excess (*ee*). The reactions were performed at either 0 or –10 °C in the presence of an excess amount of the substrate. In all cases, the oxidation was selective to sulfoxide, as sulfone was not observed. Complexes **1**–**4** were used under catalytic conditions, with yields in the range 20–78% after 72 h. A superior reactivity was observed for unprotected **3** with respect to parent complexes **1** and **2** and heteropolyblue complex **4** (Table 2, Entries 1–4).[52] No *ee* was observed for such reactions, suggesting a possible activation of several W^{VI} centers on the POM surface with diverse/opposite asymmetric induction. To evaluate this hypothesis, the reaction was performed under stoichiometric conditions, by adding only 2 equivalents of H_2O_2 with respect to the POM catalyst. Also, under these conditions, **3** and **6** displayed a better performance in terms of oxidation yield (Table 2, Entries 7 and 8). The increased reactivity for such complexes may be due to amino-assisted peroxide activation through hydrogen bonding. Low *ee* values were generally obtained; however, worthy of note is the dependence of the enantioselectivity of the reaction on the nature of the PG, being opposite with the most hindered substituent **II** (Table 2, Entry 5). Complex **6** does not give any *ee*, suggesting that the stereocenter is too far from the catalytic sites. A further remark is that under either stoichiometric or catalytic conditions, the yield of the reaction increases steadily with time, whereby the kinetic trace does not present any induction time ascribable to catalyst modification (see kinetic traces obtained with **2** in the Supporting Information).

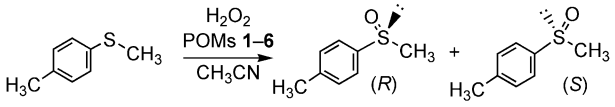

Scheme 3. Methyl *p*-tolyl sulfide oxidation with H_2O_2 catalyzed by POMs.

Table 2. Asymmetric oxidation of methyl *p*-tolyl sulfide with POMs **1**–**6** in the presence of H_2O_2.[a]

Entry	POM	*t* [h]	Yield [%][b]	*ee* [%][c]
1	(*R*,*R*)-**1**[d,e]	24	0	0
		72	35	
2	(*R*,*R*)-**2**[d]	24	9	<1 (*R*)
		72	20	
3	(*S*,*S*)-**3**[d]	24	65	0
		48	78	
4	(*S*,*S*)-**4**[d,e]	48	16	0
		72	28	
5	(*R*,*R*)-**1**	24	3	3 (*S*)
		48	21	
6	(*R*,*R*)-**2**	24	7	8 (*R*)
		72	14	
7	(*S*,*S*)-**3**	24	21	8 (*R*)
		48	59	
8	**6**	24	75	0

[a] POM (7 μmol), methyl *p*-tolyl sulfide (70 μmol), H_2O_2 (14 μmol), CH_3CN (600 μL). T = –10 °C. [b] Based on H_2O_2 content. [c] Determined by chiral HPLC. [d] POM (0.8 μmol), methyl *p*-tolyl sulfide (0.5 mmol), H_2O_2 (0.1 mmol). [e] 0 °C.

Conclusions

Surface decoration of lacunary POMs with enantiopure phosphonates yields optically active hybrid complexes that were characterized in the solid state and in solution by FTIR, heteronuclear NMR spectroscopy, mass spectrometry, and UV/Vis experiments. Furthermore, DFT calculations were performed to optimize geometries and to address the conformational stability of the different species. In such complexes, the merging of the organic and inorganic domains induces intense and multiple CD features, observed in a broad range of frequencies. Indeed the chiroptical solution behavior of the systems under investigation shows distinct Cotton effects up to 400 nm. The CD and UV/Vis spectra remain unchanged with time, indicating that the chiral hybrids are stable in solution. The chirality transfer at the POM level can be conveniently tuned as a function of the nature and structure of the organic substituents. The complexes, bearing *N*- or *O*-protected chiral amino acids, are of interest as building blocks for further functionalization and for the assembly into extended systems, including peptides or hybrid functional materials, through polymerization reactions.[20,53] Although the preliminary catalytic results are of limited synthetic interest, the oxidative activity and stability of the title complexes offer a starting point for the development of novel stereoselective catalysts. Future development in this field will also consider the use of associated chiral cations or polycations.[37]

Experimental Section

General: All reagents purchased from commercial sources were used as received without further purification. ^{1}H NMR spectra were recorded with Bruker AC250 and AV300 instruments operating, respectively, at 250.18 and 300.13 MHz. ^{13}C NMR spectra were recorded with a Bruker AV300 operating at 75.4 MHz. $Si(CH_3)_4$ was used as reference. ^{183}W NMR and ^{29}Si NMR spectra were recorded with a Bruker Avance DRX 400 instrument operating at 16.67 and 79.50 MHz, respectively, by using 2 M Na_2WO_4 in D_2O and $Si(CH_3)_4$ in $CDCl_3$ as external references. ^{31}P NMR spectra were recorded with a Bruker AV 300 instrument operating at 121.50 MHz by using 85% H_3PO_4 in H_2O as external reference. FTIR (KBr) spectra were collected with a Thermo Quest Nicolet 5700 instrument. Mass spectra (ESI) were obtained with an Agilent LC/MSD Trap SL spectrometer by using a capillary potential of 1500 V. CD spectra were recorded with a Jasco J-715 polarimeter with 1 cm quartz cells. An HPLC Shimadzu LC-10 AT VP instrument was used to detect methyl *p*-tolyl sulfoxide enantiomers. A Shimadzu GC-2010 instrument was used to measure methyl *p*-tolyl sulfide conversion. Vacant polyoxotungstates were prepared as described in the literature.[54]

(*S*)- and (*R*)-$C_{13}H_9CH_2OC(O)NHCH(CH_3)PO(OH)_2$ (II): In a round-bottomed flask, 1-aminoethylphosphonic acid (**I**; 500 mg, 4 mmol) was dissolved in H_2O (1.5 mL). K_2CO_3 (424 mg, 4 mmol) was introduced to obtain pH 8.5 and dioxane (3 mL) was then added. Separately, FmocCl (1.24 g, 48 mmol) was dissolved in dioxane (1.5 mL). The latter solution was added dropwise to the solution of **I**, and the resulting mixture was stirred overnight. After removal of dioxane under vacuum, the alkaline solution was mixed with ethyl ether to extract the unreacted FmocCl (3 × 6 mL). After

addition of $KHSO_4$ ($pH \leq 1$), the product was extracted with ethyl acetate (10×15 mL). The organic phase was dried with $MgSO_4$, and the solvent was removed under vacuum to afford a yellow solid (983 mg, 2.8 mmol, 71% yield). FTIR (KBr): $\tilde{\nu}$ =3299 (s), 2930 (w), 3053 (w), 3020 (w), 2998 (w), 2980 (w), 2951 (w), 2936 (w), 2891 (w), 1738 (m), 1685 (s), 1540 (s), 1477 (w), 1455 (m), 1447 (m), 1379 (m), 1308 (m), 1276 (m), 1262 (m), 1240 (m), 1194 (m), 1175 (m), 1104 (m, br.), 1080 (m), 1051 (m), 1021 (m), 1002 (m), 1005 (m), 940 (m), 932 (m), 918 (m), 762 (m), 744 (m), 731 (m), 705 (w), 641 (w, br.), 569 (w), 542 (w), 526 (m), 408 (w), 469 (m) cm^{-1}. ^1H NMR (300 MHz, [D$_6$]DMSO, 28 °C): δ = 7.88 (d, ^3J = 7.35 Hz, 2 H, Ar-H), 7.76 (t, ^3J = 6.71 Hz, 2 H, Ar-H), 7.41 (t, ^3J = 7.38 Hz, 2 H, Ar-H), 7.33 (m, 2 H, Ar-H), 4.22 (m, 3 H, CH_2O and CH), 3.75 (m, 1 H, CH), 1.23 [dd, ^3J = 7.49 Hz, ^3J(H,P) = 15.90 Hz, 3 H, CH_3] ppm. $^{13}C\{^1H\}$ NMR (75.47 MHz, [D$_6$]DMSO, 28 °C): δ = 155.6 (1 C), 143.9 (2 C), 140.7 (2 C), 127.3 (2 C), 125.4 (2 C), 120.1 (2 C), 65.8 (1 C), 46.7 (1 C), 44.3 [^1J(C,P) = 154.6 Hz, 1 C], 16.0 (1 C) ppm. $^{31}P\{^1H\}$ NMR (121.50 MHz, [D$_6$]DMSO, 28 °C): δ = 22.42 (s, 1 P) ppm. UV/Vis: λ ($\log\varepsilon$) = 195 (5.34), 266 (4.11), 289 (3.58), 300 (3.62) nm.

(*S*)- and (*R*)-$C_6H_5CH_2OCONHCH(CH_3)PO(OH)_2$ (III): To a solution of (*R*)- or (*S*)-1-aminoethylphosphonic acid (**I**; 200 mg, 1.60 mmol) dissolved in H_2O (1 mL) was added a solution of benzyloxycarbonyl succinimide (400 mg, 1.61 mmol) in acetonitrile (400 μL) whilst stirring. Triethylamine (300 μL) was used to achieve and maintain pH 8. After one night stirring, the organic solvent was removed under vacuum, and the remaining solution was diluted 1:1 with water. The excess amount of benzyloxycarbonyl succinimide was removed by extraction with diethyl ether (10×4 mL). The aqueous phase was acidified to $pH \leq 1$ with diluted H_2SO_4, and the product was extracted with ethyl acetate (10×8 mL). The organic layer was dried with $MgSO_4$, and the solvent was removed under vacuum to obtain the product (310 mg, 1.20 mmol, 75% yield). FTIR (KBr): $\tilde{\nu}$ = 3295 (s), 3032 (w), 2949 (w), 1689 (s, br.), 1540 (s), 1455 (m), 1428 (w), 1312 (m), 1277 (m), 1258 (m), 1225 (m), 1190 (m), 1165 (m), 1116 (m), 1082 (m), 1056 (m), 1004 (m), 941 (m), 815 (w), 779 (w), 739 (w), 714 (w), 694 (m) cm^{-1}. ^1H NMR (250 MHz, CD_3CN/[D$_6$]DMSO, 25 °C): δ = 7.32 (s, 5 H, Ar-H), 6.42 (m, 1 H, NH), 5.05 (m, 2 H, CH_2), 3.87 (m, 1 H, CH), 1.26 [dd, ^3J(H,H) = 7.32 Hz, ^3J(H,P) = 16.05 Hz, 3 H, CH_3] ppm. $^{13}C\{^1H\}$ NMR (75.47 MHz, CD_3CN/[D$_6$]DMSO, 28 °C): δ = 173.8 (1 C), 138.1 (1 C), 129.3 (2 C), 128.8 (1 C), 128.7 (2 C), 66.9 (1 C), 45.3 [^1J(C,P) = 155.43 Hz, 1 C], 26.1 (1 C) ppm. $^{31}P\{^1H\}$ NMR (121.50 MHz, CD_3CN/[D$_6$]DMSO, 28 °C): δ = 24.13 (s, 1 P) ppm. UV/Vis (CH_3CN): λ ($\log\varepsilon$): 239 (3.86) nm.

General Procedure for the Preparation of Compounds 1, 2, 5, and 8:[39] In a round-bottomed flask, $K_8[\gamma\text{-}SiW_{10}O_{36}]\cdot 12H_2O$ (500–700 mg, 0.24 mmol) was suspended in acetonitrile (15 mL) with TBABr (229 mg, 0.71 mmol). After stirring for 5 min, organophosphonic acid (2 equiv.) was added, followed by the slow addition of HCl (4 M, 4 equiv.) under vigorous stirring. The mixture was heated at reflux overnight and filtered to remove insoluble reagents and byproducts. The volume of the solution was reduced to 1 mL, upon evaporation under vacuum, than water was added to precipitate the product. The solid was finally washed with water and diethyl ether on a fritted funnel and dried several hours under vacuum.

(*R*)- and (*S*)-$(TBA)_3K[\{C_{13}H_9CH_2OC(O)NHCH(CH_3)PO\}_2(\gamma\text{-}SiW_{10}O_{36})]$ (1): $K_8[\gamma\text{-}SiW_{10}O_{36}]\cdot 12H_2O$ (700 mg, 0.24 mmol) and (*R*)- or (*S*)-**I** (165 mg, 0.48 mmol) were used to afford the product (754 mg, 83% yield). FTIR (KBr): $\tilde{\nu}$ = 2961 (m), 2932 (m), 2875 (m), 1719 (m), 1509 (m), 1483 (m), 1452 (m), 1379 (m), 1318 (w), 1267 (m), 1223 (m) 1153 (m), 1109 (m), 1051 (m), 1007 (m), 966 (s), 908 (s), 877 (s), 838 (s), 762(s), 552 (m), 457 (w) cm^{-1}. ^1H NMR (300 MHz, CD_3CN, 28 °C): δ = 7.82 (m, 4 H, Ar-H), 7.71 (m, 4 H, Ar-H), 7.38 (m, 8 H, Ar-H), 5.92 (br. d, ^3J = 9.30 Hz, 2 H, NH), 4.38–4.10 (m, 8 H, CHP, CH_2O, CH), 3.12 (m, 24 H, NCH_2), 1.62 (m, 24 H, CH_2), 1.39 (m, 30 H, CH_2 and CH_3), 0.97 (t, ^3J = 7.33 Hz, 36 H, CH_3) ppm. $^{13}C\{^1H\}$ NMR (75.47 MHz, CD_3CN, 28 °C): δ = 156.78 (2 C), 145.40 (4 C), 142.07 (4 C), 128.68 (4 C), 128.28 (4 C), 126.61 (4 C), 120.90 (4 C), 67.57 (2 C), 59.34 (12 C), 48.08 (2 C), 30.89 (2 C), 24.41 (12 C), 20.38 (12 C), 17.90 (2 C), 13.93 (12 C) ppm. $^{31}P\{^1H\}$ NMR (79.49 MHz, CD_3CN, 28 °C): δ = 20.99 (s, 2 P) ppm. ^{183}W NMR (16.67 MHz, CD_3CN/CH_3CN, 25 °C): δ = 103.11 (s, W_C, 2 W), –111.88 (s, W_A, 2 W), –113.17 (s, $W_{A'}$, 2 W), –145.11 [d, ^2J(W,P) = 8.97 Hz, W_B, 2 W], 145.24 [d, ^2J(W,P) = 8.97 Hz, $W_{B'}$, 2 W] ppm. MS (ESI–, CH_3CN): *m*/*z* = 1020. $C_{82}H_{140}KN_5O_{42}P_2SiW_{10}$ (3835.52): calcd. C 25.36, H 3.96, N 1.85; found C 26.02, H 3.70, N 1.85. UV: λ ($\log\varepsilon$) = 205 (5.18), 262 (4.74), 286 (4.38), 299 (4.33) nm.

(*R*)- and (*S*)-$(TBA)_3K[\{C_6H_5CH_2OC(O)NHCH(CH_3)PO\}_2(\gamma\text{-}SiW_{10}O_{36})]$ (2): $K_8[\gamma\text{-}SiW_{10}O_{36}]\cdot 12H_2O$ (0.7 g, 0.24 mmol) and (*R*)- or (*S*)-**II** (122 mg, 0.48 mmol) were used to afford the product (555 mg, 0.15 mmol, 63% yield). FTIR (KBr): $\tilde{\nu}$ = 3431 (br.), 2962 (m), 2874 (w), 1717 (w), 1653 (w), 1484 (m), 1457 (w, sh.), 1384 (w), 1269 (w), 1222 (w), 1154 (w), 1059 (w), 1006 (w), 966 (s), 945 (m), 909 (s), 885 (s), 840 (s), 761 (s, br.), 546 (w, br.), 453 (w) cm^{-1}. ^1H NMR (300 MHz, CD_3CN, 28 °C): δ = 7.37 (m, 10 H, Ar-H), 5.80 (m, 2 H, NH), 5.09 (m, 4 H, CH_2), 4.00 (m, 2 H, CH), 3.13 (m, 24 H, NCH_2), 1.64 (m, 24 H, CH_2), 1.40 (m, 30 H, CH_2 and CH_3), 0.99 (t, ^3J = 7.24 Hz, 36 H, CH_3) ppm. $^{13}C\{^1H\}$ NMR (75.47 MHz, CD_3CN, 28 °C): δ = 157.15 (2 C), 138.02 (2 C), 129.43 (4 C), 128.79 (2 C), 128.63 (4 C), 67.11 (2 C), 58.42 (12 C), 45.06 [^1J(C,P) = 169.78 Hz, 2 C], 24.36 (12 C), 20.33 (12 C), 16.76 (2 C), 14.04 (12 C) ppm. $^{31}P\{^1H\}$ NMR (121.50 MHz, [D$_6$]DMSO, 28 °C): δ = 21.51 (s, 2 P) ppm. ^{183}W NMR (16.67 MHz, CD_3CN/CH_3CN, 25 °C): δ = –105.92 (s, W_C, 2 W), –114.67 (s, W_A, 2 W), –115.80 (s, $W_{A'}$, 2 W), –147.84 [d, ^2J(W,P) = 9.65 Hz, W_B, $W_{B'}$, 4 W] ppm. $^{29}Si\{^1H\}$ NMR (79.50 MHz, CH_3CN\$CD_3CN$): δ = –85.8 (s, 1 Si) ppm. MS (ESI–, CH_3CN/H_2O): *m*/*z* = 964.6. $C_{68}H_{132}KN_5O_{42}P_2SiW_{10}$ (3659.31): calcd. C 22.32, H 3.64, N 1.91; found C 22.60, H 3.67, N 1.99. UV: λ ($\log\varepsilon$) = 239 (4.46) nm.

$(TBA)_3K[\{HOC(O)CH_2PO\}_2(\gamma\text{-}SiW_{10}O_{36})]$ (5): $K_8[\gamma\text{-}SiW_{10}O_{36}]\cdot 12H_2O$ (600 mg, 0.20 mmol) and $HOC(O)CH_2PO(OH)_2$ (57 mg, 0.4 mmol) were used to afford the product (514 mg, 0.15 mmol, 75% yield). FTIR (KBr): $\tilde{\nu}$ = 2961 (m), 2936 (m), 2872 (m), 1735 (m, br.), 1654 (m, br.), 1484 (m, br.), 1380 (m), 1223 (m), 1154 (m), 1109 (m), 1068 (m), 1011 (m), 969 (m), 943 (s), 912 (s), 886 (s), 839 (m), 756 (s), 559 (m), 524 (m), 457 (m), 416 (m) cm^{-1}. ^1H NMR (300 MHz, CD_3CN, 28 °C): δ = 3.14 (m, 24 H), 2.87 [d, ^2J(H,P) = 23.02 Hz, 4 H], 1.64 (m, 24 H), 1.40 (m, 24 H), 0.99 (t, ^3J = 7.34 Hz, 36 H) ppm. $^{13}C\{^1H\}$ NMR (75.47 MHz, CD_3CN, 28 °C): δ = 167.48 (2 C), 59.01 (12 C), 36.55 [d, ^1J(C,P) = 144.50 Hz, 2 C], 24.41 (12 C), 20.40 (12 C), 13.90 (12 C) ppm. ^{31}P NMR (121.50 MHz, CD_3CN, 28 °C): δ = 17.49 [t, ^2J(P,H) = 22.90 Hz, 2 P] ppm. ^{183}W NMR (16.67 MHz, CD_3CN/CH_3CN, 25 °C): δ = –106.99 (s, W_C, 2 W), –115.60 (s, W_A, 4 W), –156.93 [d, ^2J(W,P) = 11.4 Hz, W_B, 4 W] ppm. $^{29}Si\{^1H\}$ NMR (79.49 MHz, CD_3CN/CH_3CN, 25 °C): δ = –86.4 (s, 1 Si) ppm. MS (ESI–, CH_3CN): *m*/*z* = 884. $C_{52}H_{114}KN_3O_{42}P_2SiW_{10}$ (3420.98): calcd. C 19.06, H 3.79, N 1.57; found C 18.53, H 3.39, N 1.52.

Deprotection Procedures

(*R*)- and (*S*)-$(TBA)_3K[\{NH_2CH(CH_3)PO\}_2(\gamma\text{-}SiW_{10}O_{36})]$ (3): In a round-bottomed flask, (*R*)- or (*S*)-**1** (700 mg, 0.18 mmol) was dissolved in CH_3CN (6 mL). Et_2NH (300 μL, 2.9 mmol) was added.

The pale-green solution was stirred at room temperature for 1 h, following Fmoc removal by TLC (Et_2O/petroleum ether, 8:4). The mixture was concentrated to about half volume, and Et_2O/CH_2Cl_2 (8:1) was added to precipitate the product, which was collected upon centrifugation. The same solvent was used to wash the solid. The product was dissolved in acetonitrile, filtered to remove insoluble particles, and dried under vacuum to afford the pure product (321 mg, 96 μmol, 53% yield). FTIR (KBr): $\tilde{\nu}$ = 2960 (m), 2934 (m), 2872 (m), 1633 (m), 1522 (w, br.), 1484 (m), 1381 (m), 1280 (w), 1156 (m), 1106 (w), 1053 (w), 1009 (w), 995 (w), 953 (m), 900 (s), 873 (s), 833 (m), 753 (s), 560 (m, br.), 470 (w) cm^{-1}. ^1H NMR (300 MHz, CD_3CN, 28 °C): δ = 6.19 (s, 4 H, NH_2 and H_2O), 4.63–4.57 (m, 2 H, CH), 3.17 (m, 24 H, NCH_2), 1.64 (m, 24 H, CH_2), 1.41 (m, 30 H, CH_2, CH_3), 0.98 (m, 36 H, CH_3) ppm. $^{13}C\{^1H\}$ NMR (75.47 MHz, CD_3CN, 28 °C): δ = 59.24 (12 C), 42.21 (2 C), 24.38 (12 C), 20.31 (12 C), 13.95 (12 C), 11.44 (2 C) ppm. $^{31}P\{^1H\}$ NMR (79.49 MHz, CD_3CN, 28 °C): δ = 18.84 (s, 2 P) ppm. $C_{52}H_{120}KN_5O_{38}P_2SiW_{10}$ (3391.05): calcd. C 18.42, H 3.57, N 2.07; found C 20.54, H 4.00, N 2.47.

(*R*)- and (*S*)-(TBA)$_3$K[{NH$_2$CH(CH$_3$)PO}$_2$(γ-SiW$_{10}$O$_{36}$)] (4): (*R*)- or (*S*)-**2** (70 mg, 19 μmol) was dissolved in anhydrous DMF (1 mL) under an atmosphere of nitrogen. Pd/C (5.10 mg, 4.8 μmol) was added while fluxing N_2 for 5 min. A tank of hydrogen was connected with the reactor and slow bubbling of hydrogen was continued for about 2 h. The catalyst was removed upon filtration through a membrane. Et_2O/CH_2Cl_2 (8:1) was added to the resulting blue solution to precipitate the product, which was collected by centrifugation. The same solvent was used to wash the solid. The product was dissolved in acetonitrile, filtered to remove insoluble particles, and dried under vacuum to afford the pure product (26 mg, 8 μmol, 41% yield). FTIR (KBr): $\tilde{\nu}$ = 2960 (m), 2923 (m), 2872 (m), 1709 (w), 1661 (w), 1626 (m), 1382 (m), 1261 (w), 1217 (w), 1175 (w), 1016 (m, br.), 966 (s), 932 (m), 908 (m), 879 (s), 837 (m), 995 (w), 798 (m, br.), 756 (s), 873 (s), 555 (m, br.), 453 (w) cm^{-1}.

General Procedure for the Preparation of Compounds 6, 7, and 9: To a 100-mL round-bottomed flask containing a solution of (TBA)$_3$-K[{HOC(O)CH$_2$PO}$_2$(γ-XW$_{10}$O$_{36}$)] with X = Si, Ge (600 mg, 0.17 mmol) in anhydrous CH_3CN (3 mL) was added HOBT (52.2 mg, 0.39 mmol). The flask was placed in an ice bath at 0 °C. EDC/HCl (108 mg, 0.56 mmol) and triethylamine (78 μL, 0.56 mmol) were dissolved in acetonitrile (3 mL) and slowly added to the first solution. The mixture was stirred for 45 min. A solution containing H-Val-OMe·HCl (0.39 mmol) and triethylamine (54 μL, 0.39 mmol) in acetonitrile (3 mL) was added dropwise to the reaction mixture. After 90 min of stirring at room temperature, the mixture was filtered, and concentrated under vacuum. The product was obtained upon precipitation with water, washing with water and diethyl ether. Finally, it was dried under vacuum for several hours. An analogous procedure, on a smaller scale, was applied for the synthesis of **7** (with H-Phe-OMe·HCl).

(TBA)$_3$K[{CH$_3$OC(O)CH[CH(CH$_3$)$_2$]NHCOCH$_2$PO}$_2$SiW$_{10}$O$_{36}$] (6): The product was obtained in 84% yield (512 mg, 0.14 mmol). FTIR (KBr): $\tilde{\nu}$ = 2961 (m), 2928 (m), 2874 (m), 1740 (m), 1671 (m), 1541 (m), 1483 (m), 1465 (m), 1381 (w), 1262 (m), 1206 (m) 1156 (m), 1063 (m), 1010 (m), 966 (m), 942 (m), 910 (s), 884 (s), 836 (m),803 (m), 754 (s), 556 (m, br.), 522 (m), 482 (w), 455 (m), 413 (m) cm^{-1}. ^1H NMR (300 MHz, CD_3CN, 28 °C): δ = 6.77 (br. d, ^3J = 7.81 Hz, 2 H, NH), 4.29 (m, 2 H, CH), 3.69 (s, 6 H, CH_3O), 3.13 (m, 24 H, NCH_2), 2.95–2.75 (m, 4 H, CH_2P), 1.63 (m, 24 H, CH_2), 1.46–1.28 (m, 26 H, CH_2 and CH), 0.98 [m, 48 H, CH_3 (*n*Bu) and CH_3 (Val)] ppm. $^{13}C\{^1H\}$ NMR (75.47 MHz, CD_3CN, 28 °C): δ = 172.80 (2 C), 165.33 (2 C), 60.52 (2 C), 59.39 (12 C), 52.49 (2 C), 38.88 [^1J(C,P) = 140.46 Hz, 2 C], 31.73 (2 C), 24.40 (12 C), 20.40 (12 C), 19.21 (2 C), 18.60 (2 C), 13.91 (12 C) ppm. $^{31}P\{^1H\}$ NMR (79.49 MHz, CD_3CN, 28 °C): δ = 19.69 (s, 2 P) ppm. MS (ESI–, CH_3CN): m/z = 960. $C_{64}H_{136}N_5O_{44}P_2SiW_{10}$ (3608.20): calcd. C 21.25, H 3.85, N 2.35; found C 21.39, H 3.79, N 1.95. UV: λ (logε) = 192 (5.31), 261 (4.56) nm.

General Procedure for the Oxidation of Methyl *p*-Tolyl Sulfide with H$_2$O$_2$: In a jacketed reactor, cooled by circulating external ethanol, the POM-based catalyst (see Table 2) was dissolved in CH_3CN (600 μL) containing methyl *p*-tolyl sulfide (10 μL, 70 μmol). 35% H_2O_2 (0.1 mmol) was added to the cold reaction mixture. Samples were withdrawn at fixed time intervals, diluted with CH_2Cl_2, containing supported triphenylphosphane and analyzed by GC (Equity-5 capillary column; carrier He, 0.65 mL min^{-1}; T_1: 70 °C × 1 min; rate: 45 °C min^{-1}; T_2: 180 °C × 2 min; T_{inj}: 200 °C; $T_{det.}$: 280 °C; r.t.): t_R = 3.12 (methyl *p*-tolyl sulfide), 4.23 min (methyl *p*-tolyl sulfoxide) and chiral HPLC [(*S*,*S*)-DACH-DNB column; 25 cm × 4.6 mm; CH_2Cl_2/*i*PrOH, 96:4; 1 mL min^{-1}; λ = 254 nm; r.t.]: t_R (methyl *p*-tolyl sulfoxide) = 8.1 [*R*(+)], 9.5 min [*S*(–)].

Computational Details: Computational resources were provided by the Laboratorio Interdipartimentale di Chimica Computazionale (LICC) at the Department of Chemical Sciences of the University of Padova. DFT calculations were carried out by using the Amsterdam Density Functional program (ADF2007).[55] Scalar relativistic effects were taken into account by means of the two-component zero-order regular approximation method (ZORA),[56] adopting the Becke 88 exchange plus the Perdew 86 correlation functional (BP).[57] The basis functions for describing the valence electrons are triple-zeta quality, doubly polarized (TZ2P), specially optimized for ZORA calculations. Core electrons (C 1s, N 1s, O 1s, Si 1s to 2sp, P 1s to 2sp, W 1s to 4spdf) were kept frozen. The solvent effect was modeled by means of the ADF implementation[58] of the COSMO method;[59] this method requires a prior definition of the atomic radii, which were set at their following recommended values (Å): H 1.3500; C 1.7000; N 1.6083; O 1.5167; Si 1.9083; P 1.8500; W 1.9917.

Supporting Information (see footnote on the first page of this article): Spectra not reported in the paper, kinetic traces, and optimized geometries.

Acknowledgments

Financial support from the Consiglio Nazionale delle Ricerche (CNR), Ministero dell'Istruzione dell'Università e della Ricerca (MIUR), and University of Padova (PRAT CPDA084893/08) is gratefully acknowledged. Luca Sandei is acknowledged for preliminary experiments.

[1] a) M. T. Pope, A. Müller (Eds.), *Polyoxometalate Chemistry from Topology via Self-Assembly to Applications*, Kluwer Academic Publishers, Dordrecht, The Netherlands, **2001**; b) J. J. Borrás-Almenar, E. Coronado, A. Müller, M. T. Pope (Eds.), *Polyoxometalate Molecular Science*, Kluwer Academic Publishers, Dordrecht, The Netherlands, **2003**; c) D. L. Long, E. Burkholder, L. Cronin, *Chem. Soc. Rev.* **2007**, *36*, 105–121.

[2] a) K. Kamata, K. Yonehara, Y. Sumida, K. Yamaguchi, S. Hikichi, N. Mizuno, *Science* **2003**, *300*, 964–966; b) A. Sartorel, M. Carraro, A. Bagno, G. Scorrano, M. Bonchio, *Angew. Chem. Int. Ed.* **2007**, *46*, 3255 –3258.

[3] a) M. Bonchio, M. Carraro, G. Scorrano, U. Kortz, *Adv. Synth. Catal.* **2005**, *347*, 1909–1912; b) M. Bonchio, M. Carraro, A.

Farinazzo, A. Sartorel, G. Scorrano, U. Kortz, *J. Mol. Catal. A* **2007**, *262*, 36–40; c) A. Sartorel, M. Carraro, R. De Zorzi, S. Geremia, N. D. McDaniel, S. Bernhard, G. Scorrano, M. Bonchio, *J. Am. Chem. Soc.* **2008**, *130*, 5006–5007.
[4] A. Proust, R. Thouvenot, P. Gouzerh, *Chem. Commun.* **2008**, 1837–1852.
[5] M. Carraro, L. Sandei, A. Sartorel, G. Scorrano, M. Bonchio, *Org. Lett.* **2006**, *8*, 3671–3674.
[6] a) D. A. Judd, J. H. Nettles, N. Nevins, J. P. Snyder, D. C. Liotta, J. Tang, J. Ermolieff, R. F. Schinazi, C. L. Hill, *J. Am. Chem. Soc.* **2001**, *123*, 886–897; b) S. Shigeta, S. Mori, E. Kodama, J. Kodama, K. Takahashi, T. Yamase, *Antiviral Res.* **2003**, *58*, 265–271; c) X. Wang, J. Liu, M. T. Pope, *Dalton Trans.* **2003**, 957–960; d) Y. Tajima, *Microbiol. Immunol.* **2003**, *47*, 207–212.
[7] C. Sanchez, G. J. de Soler-Illia, F. Ribot, T. Lalot, C. R. Mayer, V. Cabuil, *Chem. Mater.* **2001**, *13*, 3061–3083.
[8] P. Gouzerh, A. Proust, *Chem. Rev.* **1998**, *98*, 77–112.
[9] Z. Peng, *Angew. Chem. Int. Ed.* **2004**, *43*, 930–935.
[10] J. R. Longa, O. M. Yaghib, *Chem. Soc. Rev.* **2009**, *38*, 1213–1214.
[11] Z. Zhang, Y. F. Song, L. Cronin, T. Liu, *J. Am. Chem. Soc.* **2008**, *130*, 14408–14409.
[12] M. Carraro, A. Sartorel, G. Scorrano, C. Maccato, M. H. Dickman, U. Kortz, M. Bonchio, *Angew. Chem. Int. Ed.* **2008**, *47*, 7275–7279.
[13] C. R. Mayer, R. Thouvenot, *Chem. Mater.* **2000**, *12*, 257–260.
[14] S. Nlate, L. Plault, D. Astruc, *Chem. Eur. J.* **2006**, *12*, 903–914.
[15] a) S. Favette, B. Hasenknopf, J. Vaissermann, P. Gouzerh, C. Roux, *Chem. Commun.* **2003**, 2664–2665; b) Z. H. Peng, *Angew. Chem. Int. Ed.* **2004**, *43*, 930–935.
[16] C. R. Mayer, S. Neveu, V. Cabuil, *Angew. Chem. Int. Ed.* **2002**, *41*, 501–503.
[17] a) M. Bonchio, M. Carraro, G. Scorrano, E. Fontananova, E. Drioli, *Adv. Synth. Catal.* **2003**, *345*, 1119–1126; b) M. Carraro, M. Gardan, G. Scorrano, E. Drioli, E. Fontananova, M. Bonchio, *Chem. Commun.* **2006**, 4533–4535.
[18] M. Bonchio, M. Carraro, A. Bagno, G. Scorrano, *Adv. Synth. Catal.* **2004**, *346*, 648–654.
[19] a) I. Bar-Nahum, R. Neumann, *Chem. Commun.* **2003**, 2690–2691; b) I. Bar-Nahum, H. Cohen, R. Neumann, *Inorg. Chem.* **2003**, *42*, 3677–3684.
[20] K. Micoine, B. Hasenknopf, S. Thorimbert, E. Lacôte, M. Malacria, *Angew. Chem. Int. Ed.* **2009**, *48*, 3466–3468.
[21] a) J. Schemberg, K. Schneider, U. Demmer, E. Warkentin, A. Müller, U. Ermler, *Angew. Chem. Int. Ed.* **2007**, *46*, 2408–2413; corrigendum: *Angew. Chem. Int. Ed.* **2007**, *46*, 2970; b) G. Zhang, B. Keita, C. T. Craescu, S. Miron, P. de Oliveira, L. Nadjo, *Biomacromolecules* **2008**, *9*, 812–817.
[22] J. Li, S. Hu, S. Luo, J.-P. Cheng, *Eur. J. Org. Chem.* **2009**, 132–140.
[23] a) B. Hasenknopf, K. Micoine, E. Lacôte, S. Thorimbert, M. Malacria, R. Thouvenot, *Eur. J. Inorg. Chem.* **2008**, 5001–5013; b) H. T. Evans, J. S. Showell, *J. Am. Chem. Soc.* **1969**, *91*, 6881–6882; c) J. Fuchs, R. Palm, *Z. Naturforsch. B: Chem. Sci.* **1988**, *43*, 1529–1537; d) C. M. Tourné, G. F. Tourné, F. Zonnevijlle, *J. Chem. Soc., Dalton Trans.* **1991**, 143–155; e) K. Nomiya, R. Kobayashi, M. Miwa, T. Hori, *Polyhedron* **1984**, *3*, 1071–1076; f) J. F. Garvey, M. T. Pope, *Inorg. Chem.* **1978**, *17*, 1115–1118.
[24] D. Laurencin, R. Villanneau, A. Proust, A. Brethon, I. W. C. E. Arends, R. A. Sheldon, *Tetrahedron: Asymmetry* **2007**, *18*, 367–371.
[25] H. Q. Tan, Y. G. Li, Z. M. Zhang, C. Qin, X. L. Wang, E. B. Wang, Z. M. Su, *J. Am. Chem. Soc.* **2007**, *129*, 10066–10067.
[26] Y. Hou, X. Fang, C. L. Hill, *Chem. Eur. J.* **2007**, *13*, 9442–9447.
[27] a) M. Inoue, T. Yamase, *Bull. Chem. Soc. Jpn.* **1996**, *69*, 2863–2868; b) D. L. Long, P. Kögerler, L. J. Farrugia, L. Croning, *Chem. Asian J.* **2006**, *1*, 352–357; c) X. K. Fang, T. M. Anderson, C. L. Hill, *Angew. Chem. Int. Ed.* **2005**, *44*, 3540–3544; d) X. K. Fang, T. M. Anderson, Y. Hou, C. L. Hill, *Chem. Commun.* **2005**, 5044–5046; e) L. M. Zheng, T. Whitfield, X. Wang, A. J. Jacobson, *Angew. Chem. Int. Ed.* **2000**, *39*, 4528–4531; f) H. Q. Tan, Y. G. Li, Z. M. Zhang, C. Qin, X. L. Wang, E. B. Wang, Z. M. Su, *J. Am. Chem. Soc.* **2007**, *129*, 10066–10067.
[28] a) F. Hussain, U. Kortz, *Chem. Commun.* **2005**, 1191–1193; b) V. Artero, D. Laurencin, R. Villanneau, R. Thouvenot, P. Herson, P. Gouzerh, A. Proust, *Inorg. Chem.* **2005**, *44*, 2826–2835.
[29] a) M. Inoue, T. Yamase, *Bull. Chem. Soc. Jpn.* **1995**, *68*, 3055–3063; b) U. Kortz, M. G. Savelieff, F. Y. A. Ghali, L. M. Khalil, S. A. Maalouf, D. I. Sinno, *Angew. Chem. Int. Ed.* **2002**, *41*, 4070–4073.
[30] a) C. Streb, D. L. Long, L. Croning, *Chem. Commun.* **2007**, 471–473; b) H. Y. An, E. B. Wang, D. R. Xiao, Y. G. Li, Z. M. Su, L. Xu, *Angew. Chem. Int. Ed.* **2006**, *45*, 904–908.
[31] a) Y. Q. Lan, S. L. Li, Z. M. Su, K. Z. Shao, J. F. Ma, X. L. Wang, E. B. Wang, *Chem. Commun.* **2008**, 58–60; b) Y. Q. Lan, S. L. Li, X. L. Wang, K. Z. Shao, D. Y. Du, Z. M. Su, E. B. Wang, *Chem. Eur. J.* **2008**, *14*, 9999–10006.
[32] a) N. Avarvari, J. D. Wallis, *J. Mater. Chem.* **2009**, *19*, 4061–4076; b) E. Coronado, J. R. Galan-Mascaros, *J. Mater. Chem.* **2005**, *15*, 66–74; c) P. Gerbier, N. Domingo, J. Gómez-Segura, D. Ruiz-Molina, D. B. Amabilino, J. Tejada, B. E. Williamson, J. Veciana, *J. Mater. Chem.* **2004**, *14*, 2455–2460.
[33] S. Bareyt, S. Piligkos, B. Hasenknopf, P. Gouzerh, E. Lacôte, S. Thorimbert, M. Malacria, *J. Am. Chem. Soc.* **2005**, *127*, 6788–6794.
[34] M. Lu, J. Kang, D. Wang, Z. Peng, *Inorg. Chem.* **2005**, *44*, 7711–7713.
[35] R. L. Augustine, S. K. Tanielyan, N. Mahata, Y. Gao, A. Zsigmond, H. Yang, *Appl. Catal., A* **2003**, *256*, 69–76.
[36] X. Fang, T. M. Anderson, C. L. Hill, *Angew. Chem. Int. Ed.* **2005**, *44*, 3540–3544.
[37] M. McCann, K. Maddock, *Polyhedron* **1994**, *13*, 3153–3158.
[38] C. Jahier, S. Nlate, M. Cantuel, N. D. McClenaghan, T. Buffeteau, D. Cavagnat, F. Agbossou, M. Carraro, M. Bonchio, *Chem. Eur. J.* **2009**, *15*, 8703–8708.
[39] C. R. Mayer, P. Herson, R. Thouvenot, *Inorg. Chem.* **1999**, *38*, 6152–6158.
[40] Although great effort has been made in growing single crystals of the title complexes, good-quality single crystals have not yet been obtained.
[41] J. Crassous, *Chem. Soc. Rev.* **2009**, *38*, 830–845 and references cited therein.
[42] G. Lenoble, B. Hasenknopf, R. Thouvenot, *J. Am. Chem. Soc.* **2006**, *128*, 5735–5744.
[43] a) F. B. Xin, M. T. Pope, *J. Am. Chem. Soc.* **1996**, *118*, 7731–7736; b) R. Acerete, J. Server-Carrió, *J. Am. Chem. Soc.* **1990**, *112*, 9386–9387.
[44] The paramagnetism of the species hampered the collection of ^{183}W NMR spectroscopic data.
[45] E. Papaconstantinou, A. Mylonas, *Polyhedron* **1996**, *15*, 3211–3217.
[46] E. Murguly, T. B. Norsten, N. R. Branda, *Angew. Chem. Int. Ed.* **2001**, *40*, 1752–1755.
[47] Product **6** was thoroughly washed with water and diethyl ether.
[48] The weak blue color of complexes **6** and **7** reveals that a partial reduction of the complexes occurred in such conditions, thus hampering the collection of well-resolved ^{183}W NMR spectra.
[49] J. Server-Carrió, J. Bas-Serra, M. E. Gonzàlez-Nuñez, A. Garcìa-Gastaldi, G. B. Jameson, L. C. W. Baker, R. Acerete, *J. Am. Chem. Soc.* **1999**, *121*, 977–984.
[50] A. Sartorel, M. Carraro, A. Bagno, G. Scorrano, M. Bonchio, *J. Phys. Org. Chem.* **2008**, *21*, 596–602.
[51] S. Berardi, M. Bonchio, M. Carraro, V. Conte, A. Sartorel, G. Scorrano, *J. Org. Chem.* **2007**, *72*, 8954–8957.
[52] Reduced complex **4** was much less reactive, likely because of induced radical H_2O_2 decomposition pathways.

[53] S. Monge, X. Zhang, O. Giani, J.-J. Robin, *React. Funct. Polym.* **2009**, *69*, 380–384.
[54] a) J. Canny, A. Tezè, R. Thouvenot, G. Hervè, *Inorg. Chem.* **1986**, *25*, 2114–2119; b) N. H. Nsouli, B. S. Bassil, M. H. Dickman, U. Kortz, B. Keita, L. Nadjo, *Inorg. Chem.* **2006**, *45*, 3858–3860.
[55] G. te Velde, F. M. Bickelhaupt, E. J. Baerends, C. Fonseca Guerra, S. J. A. van Gisbergen, J. G. Snijders, T. Ziegler, *J. Comput. Chem.* **2001**, *22*, 931–967.
[56] a) S. K. Wolff, T. Ziegler, E. van Lenthe, E. J. Baerends, *J. Chem. Phys.* **1999**, *110*, 7689–7698; b) J. Autschbach in *Calculation of NMR and EPR Parameters* (Eds.: M. Kaupp, M. Bühl, V. G. Malkin), Wiley-VCH, Weinheim, **2004**, ch. 14; c) E. van Lenthe, E. J. Baerends, J. G. Snijders, *J. Chem. Phys.* **1993**, *99*, 4597–4610; d) E. van Lenthe, *PhD Thesis*, Vrije Universiteit, Amsterdam, the Netherlands, **1996**.
[57] a) A. D. Becke, *Phys. Rev. A* **1988**, *38*, 3098–3100; b) J. P. Perdew, *Phys. Rev. B* **1986**, *33*, 8822–8824.
[58] C. C. Pye, T. Ziegler, *Theor. Chem. Acc.* **1999**, *101*, 396–408.
[59] a) A. Klamt, G. Schüürmann, *J. Chem. Soc. Perkin Trans. 2* **1993**, 799–805; b) A. Klamt, V. Jones, *J. Chem. Phys.* **1996**, *105*, 9972–9981; c) A. Klamt, *J. Phys. Chem.* **1995**, *99*, 2224–2235.

Received: July 27, 2009
Published Online: October 5, 2009

